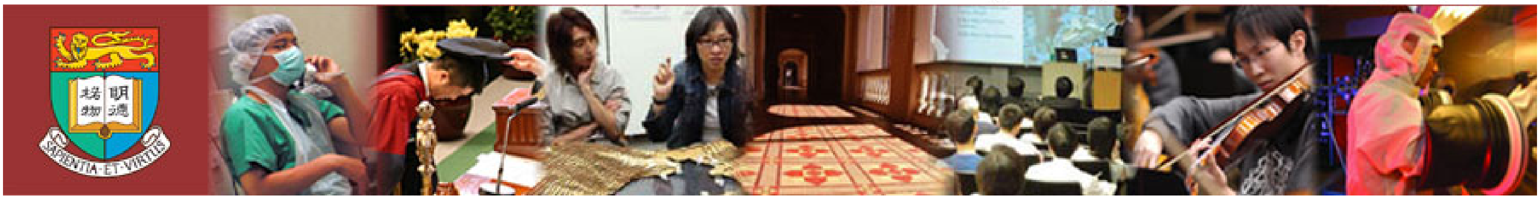

Title	Electromagnetic emissions from the IC packaging
Author(s)	Huang, NKH; Jiang, L; Yu, HC; Li, G; Xu, S.; Wang, T; Ren, HS
Citation	The 2012 IEEE Electrical Design of Advanced Packaging and Systems Symposium (EDAPS 2012), Taipei, Taiwan, 9-11 December 2012. In Electrical Design of Advanced Packaging and Systems Symposium Proceedings, 2012, p. 65-68, article no. 6469426
Issued Date	2012
URL	http://hdl.handle.net/10722/186720
Rights	Creative Commons: Attribution 3.0 Hong Kong License

Electromagnetic Emissions from the IC Packaging

Nick K. H. Huang[1], Li Jun Jiang[1], Huichun Yu[2], Gang Li[2], Shuai Xu[2], Tao Wang[3], and Huasheng Ren[2]
[1]Department of Electrical and Electronic Engineering, The University of Hong Kong
[2]Technology Planning Department, Huawei Technologies Co., LTD, yuhc@huawei.com
[3]IBM STG, East Fishkill, NY, taowang@us.ibm.com
[1]Email: khhuang@eee.hku.hk, jianglj@hku.hk

***Abstract*—The EMC and EMI of the IC packaging are becoming increasingly important to modern electronics. Its EMC, SI, and PI have been broadly attested. But electromagnetic radiations from IC packaging and the corresponding EMI were seldom studied. In this paper, the fundamental principles and properties of the electromagnetic radiations caused by vias and traces in IC packagings are carefully investigated. Various radiation mechanisms are analyzed for different representative scenarios. Numerical simulations are employed to support the analyzing results.**

***Index Terms*—EMC/EMI, radiated emission, IC packaging, trace radiation, via radiation, cavity modes**

I. Introduction

In recent decades, continuous advances in semiconductor technology pushes for improvements in integrated circuit (IC) packaging. Packaging's increasing capacities and shrinking dimensions lead to a complex electromagnetic environment. Hence, advanced modeling and optimization for multilayer packaging are needed to solve for signal/power integrity (SI/PI) and electromagnetic compatibility/interference (EMC/EMI) issues. However, most recent works have been focused on SI/PI [1]–[3]. EMI on IC packaging has become increasingly important for EMC/EMI regulations. But it was seldom studied before. Hence, the electromagnetic radiation property of IC packaging is the focus of this paper.

The radiation of the IC packaging is not an isolated problem. It is closely related to SI/PI and routing. However, to understand basic principles of complex packaging EM radiations, we intentionally separate vias and traces inside the packaging to isolate their contributions to the radiated emission. This helps us to understand the fundamental mechanisms behind the EMI of IC packaging. Numerical simulations for different representative structures are employed to interpret the complex radiation phenomena. This is an essential step before the EMI modeling of the whole packaging with all vias and traces connected. For simple canonical studies, the packaging structures are simplified into two parallel plates. Ansys HFSS is used to provide simulation results.

II. The Effects of Via Structures

The importance of fundamental via effects has been discussed in [4]. In this paper, further investigations on via structures along with a trace and a heatsink are studied.

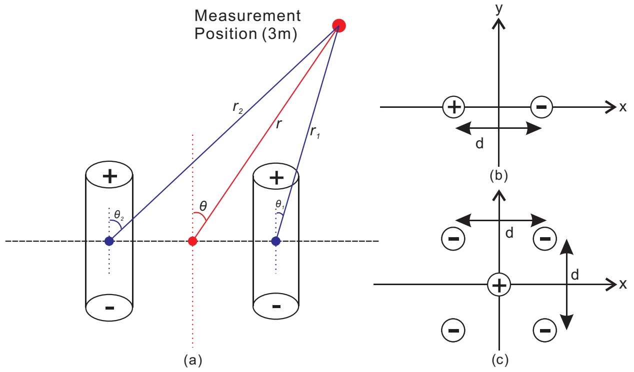

Fig. 1. (a) Vias and the measurement position. (b) Two vias with opposite currents. (c) One signal via with four surrounding GND vias.

A. The Effects of Frequency

For each via, suppose it has the current I. Its current moment is $\mathbf{P} = I_0 dl\mathbf{a}$. Even though there are top and bottom ground planes, the via can still be treated as a Hertzian dipole as Fig. 1(a) when the frequency is low. Its radiated field (when placed at the origin) is

$$E_\theta = j\omega\mu\frac{I_0 dl}{4\pi}\cdot\frac{e^{-j\beta r}}{r}\cdot\sin\theta \quad (1)$$

Hence, $E_\theta \sim O(\omega)$. When there are two vias with opposite currents (see Fig. 1(b)), the total E-field is the result of multiplication of an array factor. At low frequencies,

$$E_\theta \approx j\frac{\omega^2\mu d}{c}\frac{I_0 dl}{4\pi}\cdot\frac{e^{-j\beta r}}{r}\cdot\sin\theta\cos\varphi \quad (2)$$

Hence, $E_\theta \sim O(\omega^2)$. When there are four GND vias symmetrically surrounding the signal via in Fig. 1(c), four GND vias are assumed to share the return current. At low frequencies,

$$E_\theta \approx j\frac{\omega^3\mu d}{c^2}\frac{I_0 dl}{4\pi}\cdot\frac{e^{-j\beta r}}{r}\cdot\sin\theta\cdot\frac{d^2}{8}\cos^2(\varphi) \quad (3)$$

Hence, $E_\theta \sim O(\omega^3)$. In general, the total E-field will increase by 20, 40, and 60 dB for one order of frequency increase for one, two, and five vias, respectively.

The above analysis is only valid for low frequencies. If $d \approx 2$ mm, $\beta d \ll 1, \lambda_0 = 20\pi d$, we have $f_0 = c/\lambda_0 \approx 2.39$ GHz. Hence, this analysis is invalid above 2.4 GHz. Beyond this frequency, the approximated dipole radiation mechanism

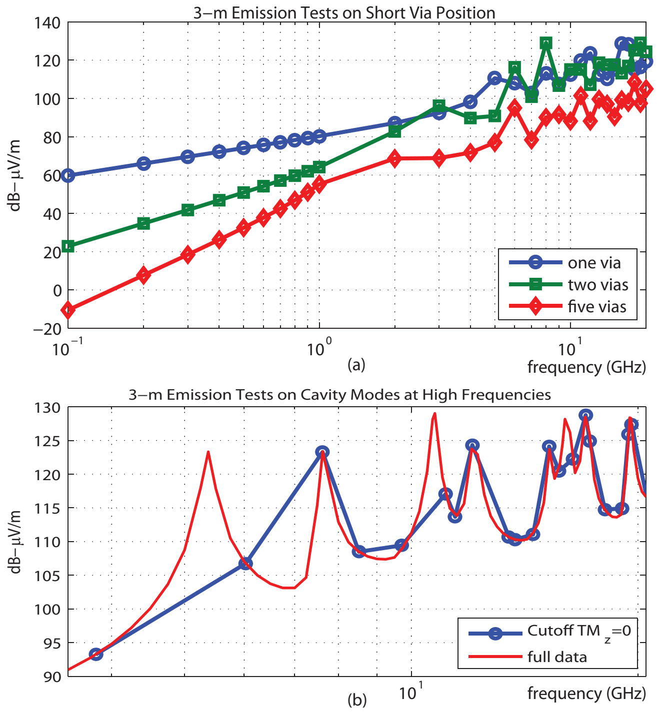

Fig. 2. 3-m emission tests (a) for short vias and (b) cavity modes at high frequencies.

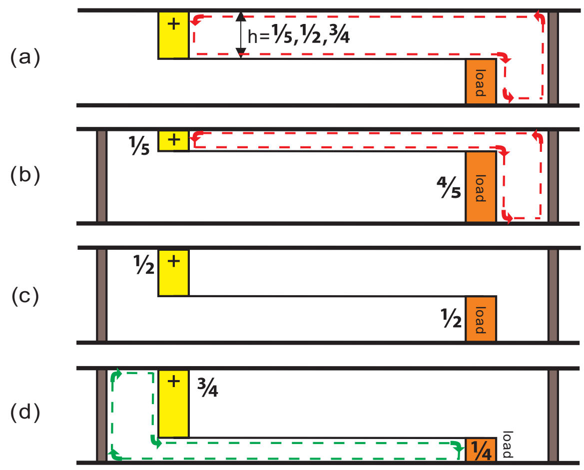

Fig. 3. A stripline structure. (a) Cross sectional view of the signal path with the trace h below the top plate. Only one ground via is used at the right of the load. (b) The signal path at height of $H/5$ when there are two ground vias. (c) The signal path at height of $H/2$ when there are two ground vias. (d) The signal path at height of $3H/4$ when there are two ground vias.

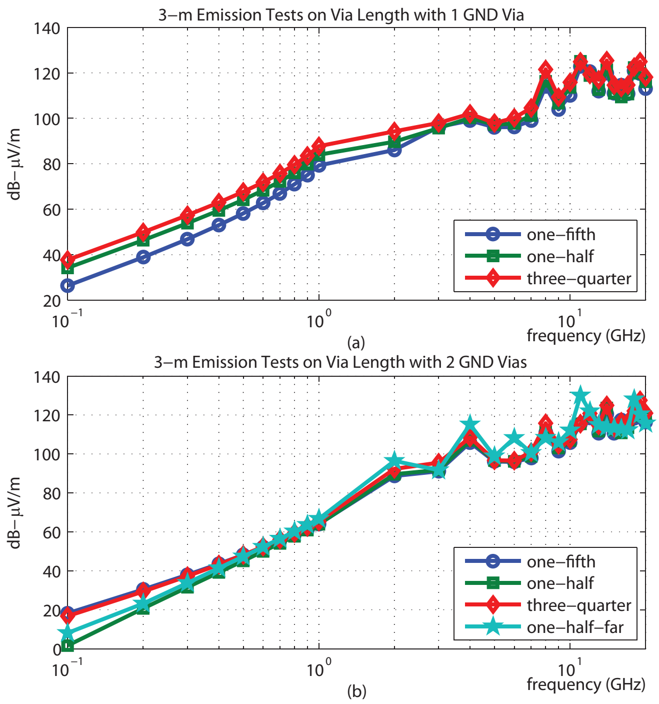

Fig. 4. 3-m emission tests for (a) 1 GND via case and (b) 2 GND vias case.

is not accurate anymore. The effects of the top and bottom ground planes have to be considered. Plus, the parallel metal plates form cavities that support the cavity modes excited by vias.

The emission tests at 3 meters are shown in Fig. 2(a). It is observed that the radiated emissions are increasing approximately at the rate of 20 dB for one via, at the rate of 40 dB for two vias, and at the rate of 60 dB for five vias at frequencies below 2.39 GHz. It proved the low frequency radiation models for vias in packaging. When vias are placed irregularly, the return currents will make the effective via configuration close to one of these three cases. Hence, at low frequencies, the increasing rate of the radiation shall be below 60 dB. More frequently, we shall see 20 dB in practical implementations.

At high frequencies, the metallic cavity with dielectrics is dominated by cavity modes: TE^z and TM^z modes. TM^z modes' cutoff frequencies can be estimated by:

$$f_{TM^z_{mnp}} = \frac{1}{2\pi\sqrt{\mu\epsilon}}\sqrt{\left(\frac{m\pi}{a}\right)^2 + \left(\frac{n\pi}{b}\right)^2 + \left(\frac{p\pi}{c}\right)^2} \quad (4)$$

where $m = 0, 1, 2, \cdots; n = 1, 2, 3, \cdots; p = 0, 1, 2, \cdots$. Similar equations can be obtained for TE^z modes. Physically TM^z modes shall be dominant in the layered packaging structure. Mathematically the lowest TE^z cutoff frequency is calculated to be above 100 GHz for the target structure, which is much higher than that of the first TM^z mode. The cutoff frequencies of TM^z modes when $p = 0$ are calculated and shown in Fig. 2(b). It reveals many correlations between the cutoff frequencies of cavity modes and the peak radiation of the packaging at frequencies from 3.5 to 20.5 GHz. It is also observed that the estimated cavity cutoff frequencies are not necessarily at the resonance. There are some other radiation peaks that need further study and understanding.

B. The Position of the Stripline in the Package Layers

The position of a stripline is an important factor to the contribution of EMI. It is interesting to find out how it affects the IC packaging EMI.

Figure 3 illustrates a stripline structure with different po-

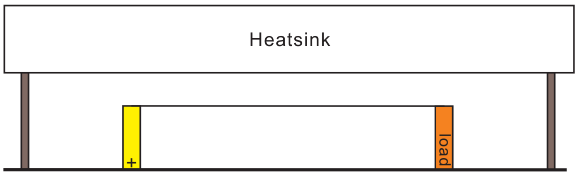

Fig. 5. A microstrip line structure with a heatsink on top of it.

sitions. Their radiated emissions are simulated at 3-meter measurement position. The first case is only one GND via is present next to the load on the right, as shown in Fig. 3(a). The whole structure then becomes a loop around the top and bottom plates. The loop size is determined by the height h. The radiation results are shown in Fig. 4(a) for $h = H/5$, $H/2$, or $3H/4$, where H is the gap between two parallel plates. Apparently $H/5$ case has the lowest radiated emissions since it has the smallest current loop area (see 3(b) red loop). The highest radiation occurs in the case of $3H/4$.

The 2-GND-via structure is performed for three different trace positions with simulated results displayed in Fig. 4(b). Two loops are formed thus the overall radiated emissions are less than one GND via cases because of current loop cancellations. The lowest radiation happens when both loops have around the same areas to cause the balanced cancellation, which is for the $H/2$ case. Another interesting point for the balanced $H/2$ case is to move the right GND via further away from the load via. Then the return current loop will become larger to cause unbalanced radiation for two current loops. Hence, higher radiated emissions (Fig. 4(b) last curve) is expected. It means when one GND via presents, a smaller loop area is preferred to cause less radiations. When two GND vias present, a balanced arrangement is preferred. But at very high frequencies, the radiation of all cases are similar. This tells that the cavity mode radiations become dominant.

C. The Effects of the Heatsink on the Microstrip

A microstrip line is a common transmission line structure. It is chosen here to investigate the effect of a heatsink structure to the packaging radiation.

Fig. 5 shows the structure of a microstrip line and a heatsink. The heatsink is simply grounded to the ground plane of the microstrip line at the four corners of the heatsink. It is seen that at the low frequency range, the existence of the heatsink actually reduces the radiation. But at the high frequency range, the radiation with heatsink increases. It is also obvious that the high frequency behavior with the heatsink is more oscillatory. It means that the heatsink forms a new cavity that dominates the high frequency radiation. In reality co-planar waveguide (CPW) is often used. Adding a heatsink to the CPW on packaging will exhibit similar behavior.

III. The Effects of Trace Structures

The trace radiation mechanism plays an important role in the IC packaging EMC/EMI. Different trace structures are studied for their radiation effects in the packaging.

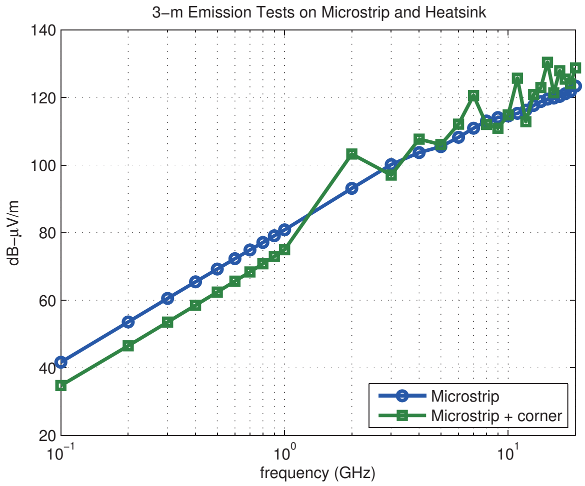

Fig. 6. 3-m emission tests on the microstrip line and the heatsink.

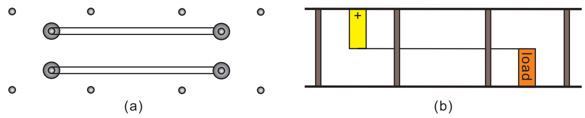

Fig. 7. A differential traces structure. (a) top view. (b) cross-sectional view.

A. Differential Traces

Two differential traces structures are studied and compared. The first one is shown in Fig. 7 with four GND vias surrounding each signal via. The second case is when there are only four GND vias and they are placed at the four corners of the packaging, far away from signal vias. The 3-m measurement position is taken to obtain the maximum emission tests shown in Fig. 8.

From the results of the first case, the differential mode of differential traces has higher radiated emissions than the common mode at low frequencies below 0.4 GHz. Above 0.4 GHz, the differential mode has lower radiations than the common mode, and this is expected. The reasons for the low frequency distortion is due to the location of the GND vias. At the common mode, the two signal vias on the one side act as one signal via and the surrounding four GND vias are the path to share the return current. As a result, it increases by 60 dB for one order of frequency increase [4]. At the differential mode, the two vias have the opposite currents, and the surrounding GND vias join one of the signal vias to share the current path. Therefore, the radiation increases by 40 dB for one order of frequency increase. This is only valid at low frequencies.

The illustration of Fig. 8 shows a reasonable result that the differential mode has lower radiations than the common mode overall. The differential mode can be explained in similar details in last case. For the common mode, at frequencies below 300 MHz, the two signal vias on one side are acting as one signal via, so the radiated emission increases by 20 dB for one order of frequency increase. For frequencies above 300 MHz, the four GND vias in the corner come in to play an

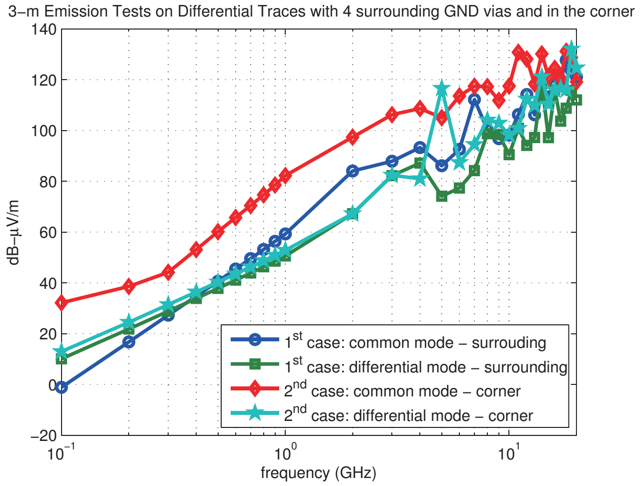

Fig. 8. 3-m emission tests on differential traces with 4 surrounding GND vias and in the corner.

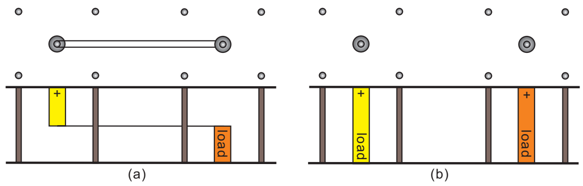

Fig. 9. Trace EMI effect test by comparing two cases: (a) with trace and (b) without trace.

important factor to make the radiated emission increase at 60 dB for one order of frequency increase. At higher frequencies, the metallic cavity modes dominate the radiation.

B. The Study between Trace and No Trace

To understand the relative contribution importance of traces and vias in packaging structures, two cases are studied and compared. Fig. 9(a) shows a trace in-between two shorted parallel plates. Both signal via and load via are surrounded by 4 GND vias that short top and bottom ground planes. In the second case shown in Fig. 9(b), the trace is removed. The vias are extended to shorted plates. To maintain the same current on two vias, in Ansys HFSS the top surface of the via is used as the wave port, and the bottom surface of the via is used as the load. To compensate the phase shift due to the length of the trace, the excitation current phase of the right via in Fig. 9(b) has a phase delay equal to the phase shift of trace in Fig. 9(a) at each frequency. Both vias in Fig. 9(b) are extended by one time to enable reasonable port and load setups.

The simulated 3-meter radiated emissions of both cases at all frequencies are shown in Fig. 10. Two emissions are almost identical except a difference of around 6 dB. It means the radiated field magnitude of Fig. 9(b) is almost exactly doubled than that of Fig. 9(a). Considering the fact that the current length of vias are doubled in Fig. 9(b), it can be seen that the trace radiation is trivial compared to that of vias.

The phenomena can be explained with several reasons. First, the TEM mode propagated along the stripline trace

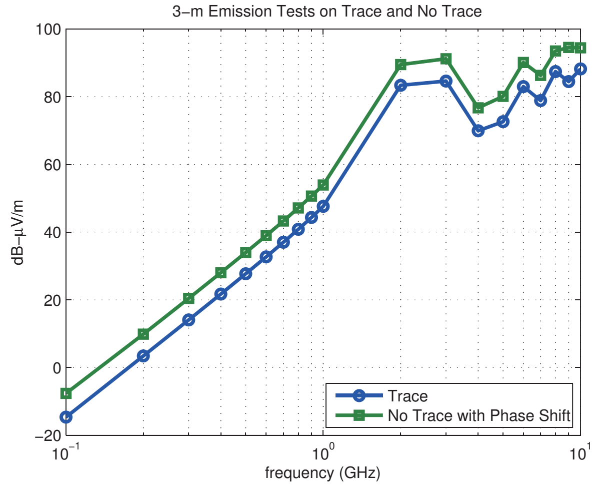

Fig. 10. 3-m emission tests on trace and no trace.

does not radiate. Secondly, TM^z modes are dominant in this type of packaging structures. But the horizontal traces are not good excitation sources for these modes. Thirdly, most guided modes by traces are absorbed by matched loads. Hence, the via EMI effects are more critical. Under this scenario, both vias and traces will work together to increase the radiated emissions of IC packaging.

IV. Conclusion

This paper studied the fundamental via and trace radiating principles of IC packaging for electromagnetic interference issues. This research area was seldom addressed but is increasingly important for today's EMI qualification and regulation. The radiation mechanisms of vias, traces, current loops, and heat sinks are carefully investigated under different scenario. It provides helpful guidance for optimal low emission IC packaging designs.

Acknowledgment

This work was sponsored by the Research Grants Council of Hong Kong (GRF 713011 AND 711511), HKU (201102160033 and 201007176196), and Huawei Technologies Co., LTD.

References

[1] F. de Paulis, Y.-J. Zhang, and J. Fan, "Signal/power integrity analysis for multilayer printed circuit boards using cascaded s-parameters," *Electromagnetic Compatibility, IEEE Transactions on*, vol. 52, no. 4, pp. 1008 –1018, nov. 2010.

[2] Y.-J. Zhang, Z. Z. Oo, X.-C. Wei, E.-X. Liu, J. Fan, and E.-P. Li, "Systematic microwave network analysis for multilayer printed circuit boards with vias and decoupling capacitors," *Electromagnetic Compatibility, IEEE Transactions on*, vol. 52, no. 2, pp. 401 –409, may 2010.

[3] R. Rimolo-Donadio, X. Gu, Y. Kwark, M. Ritter, B. Archambeault, F. de Paulis, Y. Zhang, J. Fan, H.-D. Bruns, and C. Schuster, "Physics-based via and trace models for efficient link simulation on multilayer structures up to 40 ghz," *Microwave Theory and Techniques, IEEE Transactions on*, vol. 57, no. 8, pp. 2072 –2083, aug. 2009.

[4] N. K. H. Huang, L. J. Jiang, H. Yu, G. Li, S. Xu, and H. Ren, "Fundamental components of the ic packaging electromagnetic inference (emi) analysis," in *EPEPS, 20th IEEE*, 2012.